PERGAMON

Radiation Measurements 35 (2002) 515–525

Radiation Measurements

www.elsevier.com/locate/radmeas

Radiation dose measurements aboard the Mir using the R-16 instrument

V.G. Mitricas[a,*], V.V. Tsetlin[a], M.V. Teltsov[b], V.I. Shumshurov[b]

[a] *Institute of Biomedical Problems, Moscow, Russia*

[b] *Skobeltsyn Institute of Nuclear Physics, Moscow State University, 119899 Moscow, Russia*

Received 28 August 2000

1. Introduction

Manned space flights are now an everyday practice. However, the problem of radiation safety is far from being solved and its priority is still very high. Probably, effective methods for forecasting the occurrence and evolution of solar proton events will not become available soon. For the present, there is no clear understanding of the dynamics of the absorbed dose rate induced by the protons in the Earth's radiation belt during one solar cycle, let alone of diurnal and hourly variations. There are no reliable experimental data on the influence of geomagnetic disturbances on the radiation environment in manned spacecraft orbits and, correspondingly, there is no method of estimating their influence on the radiation exposure of cosmonauts.

By the time the Mir station became operational, a certain amount of experience in the radiation safety provision of piloted spacecraft had been acquired. This experience was reflected in a system that includes:

- standards of radiation safety for piloted space flights of duration up to 3 years;
- models of radiation risk during periods of cosmonaut working activity;
- models of space radiation sources; and
- methods for calculating radiation penetration through shielding and the resultant absorbed and equivalent doses.

Subsequently, this system was extended to include:

- common requirements for the effective provision of flight radiation safety;
- examination of the flight radiation provision system, etc.

The systems of radiation safety provision are always considered as a component of the space flight biomedical provision, including the whole complex of organizing and engineering methods being carried out at the stages of designing and construction of spacecraft, during flight, and following flight. The starting point in solving this problem is in updating the radiation safety standards (State Standard, 1985) which requires knowledge of the radiation conditions during spaceflight. The basic conditions are as follows (RD, 1991):

- energy and charge spectra and angular distributions of space radiation at specific calendar times;
- ballistic characteristics of the orbit;
- shielding distributions of crew working areas inside the spacecraft;

There are four natural sources of cosmic radiation capable of making an appreciable contribution to cosmonaut absorbed dose:

- protons and electrons in the Earth's radiation belts (ERB);
- galactic cosmic ray particles (GCR);
- solar cosmic ray protons and electrons (SCR) during solar proton events (SPE);
- space and albedo neutrons;

If the characteristics of space radiation are known, other aspects of the radiation safety problem can be formulated:

- passive radiation through the Earth's magnetosphere (especially for GCR and SPE);
- radiation penetration through the shielding and instrumentation of spacecraft and through the space suit during EVA;
- formulation of the dose field inside a spacecraft and a cosmonaut's body with consideration of the working place shielding.

* Corresponding author.
E-mail address: panasyuk@srdlan.npi.msu.su (V.G. Mitricas).

PII: S1350-4487(02)00084-7

The first two sources of space radiation exhibit a slow variation with time. The most typical feature of this behavior is the change in intensity by nearly a factor of two from the period of maximum solar activity (solar maximum) to the period of minimum solar activity (solar minimum). Because of this variation, phenomenological descriptions based on a large number of experimental data sets are the most widely used models. After different types of processing, the models are presented as tables of nomograms both for the solar maximum and solar minimum phases. The problem of the source behavior approximation for these phases has not been solved completely (SS 25645.138, 1987; SS 25645.135, 1987; Vernov, 1983; Sawyer and Vette, 1976). In addition, each solar cycle has unique features and, at present, there are no models which take this into account with sufficient accuracy.

The third source has a pronounced stochastic character and the basic problem is the forecasting (long term and short term) of SPE occurrence and of the characteristics of the particular SPE proton spectrum.

The density of the space neutron flux is low and it does not contribute substantially to the absorbed dose in piloted spacecraft orbits. Albedo neutrons are created in the Earth's atmosphere after interactions of the atmosphere with GCR particles. According to estimates made in Kovalev et al. (1986), the contribution of albedo neutrons to the absorbed dose does not exceed 25–60 μSv/day.

2. Instrumentation

Despite the fact that a lot of different dosimetric instruments (TLD, IPD-2, Pille, Liulin, Nausicaa, Circe, JSC-TEPC, etc.) were used inside the piloted Mir station at different times, the basic instrument providing routine monitoring of the radiation environment inside the station was the permanently mounted R-16 dosimeter. As a rule, daily data were received from this instrument by the Space Radiation Safety Service (SRSS) and were the basis of absorbed dose measurements inside the station for nearly the whole time of the flight. The analysis of this data is presented in this paper.

The R-16 dosimeter consists of two ionization chambers of the integral-pulse type IK-5. One ionization chamber, D2, measured the absorbed dose inside the Base Block of the station. The second ionization chamber, D1, has added tissue equivalent shielding of 3.0 g/cm^2. The instrument also has a unit containing support electronics: voltage converters, pulse generators and two channels of operational memory. Each ionization chamber consists of a cylinder with a diameter of 60 mm with hemispherically shaped ends and is filled with pure argon up to pressures of 4.5×10^5 Pa. The collector for each chamber runs through the working volume, through an amber insulator, and into the support unit where a shaft-type electrostatic relay (ESR) is located. By means of the ESR the charge on the collector is picked up when a certain potential on the collector is achieved by the ionization current inside the working volume. The dose value of one pulse of the ESR was fixed during calibration at 5 mrad/pulse (50 μSv/pulse). The measurement accuracy of the absorbed dose is 5% for all types of penetrating radiation within a dose rate range of 0.4 mrad/h to 1000 rad/h. The standard chamber has a very low efficiency for neutron counting. The resource of chamber processing exceeds 10^6 pulses. The ionization has practically isotropic sensitivity and there is no dependence of the sensitivity on the hardness of soft gamma and X-ray radiation. The metrological characteristics of the chamber were studied during a special program at the Mendeleev Institute of Metrology, St. Petersburg (Yuraytin et al., 1979). It should also be mentioned that, because the operating conditions aboard the Mir station were not so strong, the working volumes of the IK-5 chambers were not air-tight. They must be air-tight for other applications, including operation in open space.

3. Database

On 13 March 1986 the crew of the first mission (EO-1) was launched to the Mir station. This also represented the last mission to the Salyut-7 station. On 15 March, after docking, the EO-1 crew moved into the Base Block of the Mir station and remained there until 5 May 1986. Because of technical difficulties, the regular receiving of telemetric information, including data from the R-16 dosimeter, only began on 28 March 1986. After the visit to the Salyut-7 station on 27 June, the crew returned to the Mir station and remained there until 15 July.

The second mission to the Mir station (EO-2) was launched on 6 February 1987 and R-16 dosimetry data transmission to Earth began on 8 February. The analysis of the received data showed that the D1 channel was not operating correctly. On 1 October 1987, the dosimeter was exchanged, but again the dose from the D1 chamber sometimes exceeded the dose from the D2 chamber. Only after a second dosimeter exchange on 30 March 1990 did the measurement results of the absorbed dose start arriving at SRSS from both channels. As a result of the daily dosimetric monitoring of the radiation environment aboard the Mir station, a prolonged series of practically constant data was received. These data allowed us to analyze the radiation dynamics during the whole of the 22nd solar cycle. During the EO-1 mission, the total time the crew lived aboard the Mir was only 71 days (only 58 days of absorbed dose data was measured). The station was unoccupied for an interval lasting 7 months prior to the launch of the EO-2 mission. Therefore, only dosimetric results beginning with the EO-2 mission are presented and analyzed in this paper.

The interval in the piloted regime of the Mir station between the EO-4 and EO-5 missions breaks up the data into two parts. The first part occurred during the period between

8 March 1987 and 26 June 1989 and included the minimum between the 21st and 22nd solar cycles. The beginning of the growth phase of the 22nd solar cycle is characterized by an orbit of average altitude of $H_{sp} = 352.39 \pm 13.86$ km. During the second part, following 7 September 1989 and including the end of the growth phase, the maximum and decline phases of the 22nd solar cycle, the minimum phase between the 22nd and 23rd solar cycles, and the beginning of the growth phase of the 23rd solar cycle, the average altitude of the orbit was $H_{sp} = 393.27 \pm 13.22$ km. As the radiation analysis shows, variation in the average altitude of the orbit was considerable.

Late in the second period, there was inconsistency in the D2 channel operation. From about August 1995 onwards, the reading from the D2 channel showed a tendency toward increased counting rate in comparison to the rate measured by the D1 channel. A possible reason for this inconsistency in the R-16 dosimeter operation could be the penetration into the working volume of the instrument of an agent that caused an increase in the frequency of ESR switching through the accumulation of additional electrostatic charge. An argument in favor of this explanation springs from the accidents on the station with the refrigerant used in the life support system and repeated increases in the temperature of the station's atmosphere. These accidents are correlated with the maximum reading in the R-16 D2 channel. After replacement on 30 April 1997, the R-16 dosimeter which had operated aboard Mir station during the previous years was returned to Earth by the NASA Space Shuttle for analysis. Ground experiments allowed us to establish that the refrigerant agent penetrated into the working volume of the D2 chamber. This refrigerant caused an additional leakage current, the refrigerant's electroconductivity increased only when the temperature exceeded 25°C. Cleaning of this volume completely restored the chamber's operation up to a temperature of 50°C. It was found that the calibration of the chamber had not changed during the 6 years of operation aboard the Mir station.

To examine the stability of the D2 channel measurement, we considered the dependence of the ratio of the D2 channel readings to the D1 channel readings as a function of time (Mitricas and Tsetlin, 2000). It turned out that, from the end of July 1985, this ratio was nearly constant with only a small, long-term trend.

We took the average value of the D2/D1 ratio for the period up to 31 July 1995 and multiplied it by the difference in the daily readings from the D1 channel. The obtained results were integrated over the number of days, rounded down to the nearest integer, and multiplied by 5 (the R-16 sensitivity was 50 μSv/pulse or 5 mrad/pulse). The difference in the rounded off values was then taken as the R-16 D2 channel readings. Correlation was made between the results from the D2 channel R-16 dosimeter readings and telemetry data from each communication cycle between 30 January 1996 and 14 March 1997 or 1156 orbits. The intermediate database was created for this analysis. This database includes the date, time, orbit number and dosimeter readings. For execution of the analysis by means of calculation, the ballistic parameter of each orbit was determined. During this analysis period, the parameters varied within the following limits: the apogee altitudes ranged from 395.5 to 413.0 km, the perigee argument varied from 2.9° to 158.6°. Using variations of the ascending node longitude, it was determined that the station passed along the near orbit once in every 46 orbits. The total duration for this number of orbits is about 3 days ($\sim$ 70.5 h). All orbits were separated in groups of 46 orbits each (25 total groups) and for each orbit in a group, the dosimeter readings were processed using a nonrecursive filter of the following form:

Using this filter method, the first part of the series is separated from the last part by 6

$$D_i^* = \frac{(D_{i-46} + 2D_i + D_{i+46})}{4}, \quad i = 1, 2, \ldots, 46 \qquad (1)$$

days and the difference in the ascending node longitudes is only 5.6°. Since Eq. (1) condition cannot be satisfied for the first and last 46 orbits, dosimeter readings from these orbits were determined as average values of the first and second groups of 46 orbits and for the last and second to last groups of 46 orbits. Among each group, the minimum reading was determined and used as the D_f background. By subtracting the D_i^* value from D_f, we obtained values which we used as real measurements of absorbed dose from the D2 channel grouped and summed by orbit according to the time of daily ballistic parameters and differences in $D_i^* - D_f$ were rounded down to the nearest integer and then multiplied by 5. The difference in the rounded-off values was used as the daily measurement of the D2 channel.

Comparison of the results obtained in this way with the results obtained by multiplying the D1 channel daily data by the average ratio of D2/D1 for the period up to 31 July 1995 shows that the two are practically the same. Nevertheless, on 30 April 1997 the R-16 dosimeter was exchanged again.

Using the results of the daily operative monitoring of the radiation environment on Mir station the database was formed and included as the follow parameters:

- the date (day/month/year);
- the time of determination of ballistic parameters (h/min/s);
- ballistics (the inclination of the orbit with respect to the equatorial plane i, the period of the orbit T, the apogee altitude H_a, the perigee altitude H_h, the longitude of the ascending node, and the perigee argument (φ);
- the daily increment of R-16 dosimeter readings from the D1 and D2 channels;
- the values of the Wolf number, W;
- the radio-frequency radiation from the Sun at a wavelength of 10.7 cm, $F_{10.7}$;
- the intensity of the GCR proton flux at $E > 90$ MeV (using data from the "Meteor" satellite until the second-quarter of 1997);

- the proton daily flux at $E > 100$ MeV (using data from the "GOES" satellite).
- the A_p-index value;
- the ring current amplitude (the D_{st} variation).

The values of the latter indices were entered into the database from both values transmitted by different codes of the International Radio Union and from Internet.

In addition, the database includes data on the average altitude of the orbit during the Mir station traversal of the South Atlantic Anomaly, H_{SAA}, and the average density of the atmosphere in this region, ρ. An estimate of the atmospheric density was made using the technique described in State Standard 25645.115 (SS 25645.115, 1985) which is based on satellite deceleration data, does not take into account the local atmospheric features, and can give incorrect results. This fact must be taken into account when using data based on the atmospheric density.

4. Absorbed doses induced by SPE protons

A number of SPEs which contributed considerably to the absorbed dose were observed over the lifetime of the Mir station especially during the 22nd solar maximum. The level of the radiation exposure of cosmonauts induced by SPE protons is determined by the following parameters:

- the proton flux intensity;
- the energy spectrum, characterized by an exponent using the power law form of the spectrum or by a characteristic steepness using the steepness form;
- the degree of station shielding by the Earth's magnetic field which strongly varies during the flight (the planetary distribution of effective vertical softness cut-off);
- the geomagnetic field conditions described by the D_{st} variation amplitude;
- protection of cosmonauts working places by local mass or by shielding functions.

Calculations show that SPEs with total proton flux at energies above 30 MeV/event lower than 10^6 protons/cm^2 can, as a rule, be neglected in the operative provision of the flight radiation safety on the Mir station. SPE with the total flux $J(>30) < 10^7$ protons/cm^2 contribute a little to the absorbed dose measured by the R-16 dosimeter and their contribution can be often classified as a result of other space-physical factors. For a significant contribution of SPE protons to the absorbed dose on Mir station, the following conditions have to be satisfied simultaneously: high intensity of the high-energy particle flux; nearness of SPE occurrence coordinates on the Sun to the optimal longitudinal interval; locations of the Earth and the Sun in the same sector of the interplanetary magnetic field inside the current sheet; passage of SPE protons through the Earth's magnetosphere against a magnetic storm, etc. As simultaneous occurrence of all these conditions seldom occurs, SPEs rarely make a reliably registered contribution to the absorbed dose. Table 1 contains several characteristics of the most powerful SPEs which illustrate the above-mentioned conditions. From Table 1 it follows that the events N 12–14 contributed considerably to the absorbed dose. It should be noted, that in October 1989 the NASA Space Shuttle "Atlantis" was also in orbit. However, the orbital inclination of "Atlantis" was 28.5° and, according to SRSS estimates even during the geomagnetic storm, protons from the 19 October 1989 SPE did not reach such low latitudes and American astronauts did not receive an additional contribution to the absorbed dose.

During the passage of protons from the 19 October 1989 SPE, recommendations were transmitted to the Mir station which requested that the cosmonauts should not leave the Base Block module or enter their cabins during the time Mir station crossed the polar caps. Due to persistent requests of the flight controllers, these recommendations were followed, and the dose acquired by the astronauts (from solar protons of the 20 October 1989 SPE) was 3 times smaller than what would have been acquired had such recommendations been not followed. It should be noted that, according to the requirements of SRSS, all the telemetry data receiving stations were put into operation, and the service received data from Mir station for most of the orbits. This permitted us to obtain a detailed picture of the absorbed dose increase inside the station, to make certain decisions, and later to perform a detailed analysis. This also gave us the opportunity to create a detailed picture of the increase in the absorbed dose inside the station (Tverskay et al., 1991).

The March 1991 SPE differed from the other events in that, for a relatively long time (over 10 days), proton fluxes with energies over 40 MeV significantly exceeded the background level. The low-energy protons could penetrate into the inner regions of the Earth's magnetosphere and, due to several magnetic storms (during 1.5 months there were 10 cases when the D_{st} index absolute value exceeded 50 gammas), could give an additional contribution to the absorbed dose. It is impossible to accurately separate out this effect because additional fluctuations of the absorbed dose dynamics caused by orbit corrections on 11 and 15 April resulted in an increase in altitude of 4 and 5 km, respectively. Using the absorbed dose dynamics after the SPE series in June 1991, an attempt was made to estimate the speed of absorbed dose decay. The dependence of absorbed dose rate on time was presented in the form (Mitricas and Tsetlin, 1995)

$$P(t) = P_0 \exp(-t/T), \tag{2}$$

where P_0 is the average daily absorbed dose for the period of 16–18 May 1991 and is equal to 45 mrad/day, t is the time in days starting on 12 May 1991, and T is the decay constant of the absorbed dose rate being sought.

After 15 June 1991, an essential orbit correction which influenced the absorbed dose rate was made on 28 August 1991 ($H_d = 71$ m) and the average dose rate was

Table 1
Several parameters of SPE during the exploitation period of the MIR station

No.	Date	Heliolongit ude	J_{30} (cm^{-2})	R_0 (MV)	$D_{CB}(1)$ (rad)	D_{st} (gamma)	D(P-16) (mrad)
1	8.XI.87	W90				−4	5 ± 5
2	5.I.88		2.14×10^6	31.8	3.2	−45	—
3	8.XI.88	W47	2.76×10^6	69.8	1.4	−45	—
4	24.XI.88		1.00×10^6	110.9	0.3	−4	—
5	14.XII.88		3.96×10^6	101.2	2.3	−32	—
6	8.III.89	E69	3.14×10^5	90.5	0.2	−23	—
	9.III.89		6.00×10^5	38.5	0.8	−68	5 ± 5
7	12.III.89	E89	4.74×10^5	34.7	0.7	−189	25 ± 5
8	17.III.89	W60	7.50×10^6	33.6	12.2	−64	40 ± 5
9	23.III.89	W28	7.12×10^6	45.5	8.0	−60	30 ± 5
10	11.IV.89	E59	1.00×10^6	24.2	2.7	−9	—
11	22.IV.89		1.49×10^6	45.5	1.7	−2	5 ± 5
12	29.IX.89	W105	1.10×10^9	87.7	472.0	−105	480 ± 5
13	19.X.89	E10	2.30×10^9	65.8	1076.0	−105	2720 ± 5
14	22.X.89	W31	1.17×10^9	65.7	568.0	−123	300 ± 5
15	24.X.89	W57	5.30×10^8	80.0	222.0	−50	140 ± 5
16	15.XI.89	W26	1.20×10^7	85.7	4.2	−18	5 ± 5
17	30.XI.89	W59	5.30×10^7	32.2	32.8	−37	—
18	19.III.90	W43	4.41×10^6	27.2	9.2	−37	—
19	21.V.90	W36	5.53×10^7	67.8	44.8	−63	10 ± 5
20	24.V.90		4.74×10^7	90.3	32.0	−29	5 ± 5
21	26.V.90		3.51×10^7	87.6	25.7	−66	—
22	28.V.90		1.18×10^6	108.5	0.7	−28	5 ± 5
23	25.VII.90		1.46×10^6	35.1	2.7	+17	—
24	23.III.91	E28	5.69×10^8	45.6	323.3	−194	245 ± 5
25	4.VI.91	E70	1.20×10^7	65.7	10.1	−15	—
26	6.VI.91		6.76×10^7	64.4	30.9	−66	10 ± 5
27	9.VI.91		1.07×10^7	44.8	6.1	−29	20 ± 5
28	11.VI.91		1.84×10^8	59.9	88.8	−197	200 ± 5
29	15.VI.91	W69	1.47×10^8	62.4	64.2	−61	70 ± 5
30	29.VI.91		2.17×10^6	34.1	1.3	−19	35 ± 5
31	1.VII.91		6.68×10^6	32.8	4.1	−10	—
32	7.VII.91	E03	4.28×10^6	24.9	2.6	−7	15 ± 5
33	26.VIII.91	E64	7.40×10^5	21.0	0.4	−95	5 ± 5
34	30.X.91	W25	5.37×10^6	88.2	2.0	−107	—
35	7.III.92		1.47×10^6	78.7	0.6	−2	—
36	8.V.92	E08	6.62×10^6	32.8	4.1	−49	5 ± 5
37	25.VI.92	W67	2.00×10^7	45.4	10.6	−3	5 ± 5
38	30.X.92	W61	2.05×10^8	43.9	122.4	−37	10 ± 5
39	2.XI.92					−41	10 ± 5
40	20.II.94	W02				−30	10 ± 5
41	6.XI.97	W63				−62	40 ± 5

E(W)—the eastern (western) heliolongitude; $J(30)$—the proton total flux at $E > 30$ Mev per event; R_0—the characteristic steepness of the proton spectrum, MV; $D_{CB}(1)$—the estimation of the absorbed dose in free space beyond the shielding of 1 g/cm^2; D_{st}—the average daily value of D_{st} the day of the SPE flux maximum; D(R-16)—the estimation of the dose's contribution induced by SPE using the R-16 dosimeter date (the error of determination is taken to be equal to the R-16 sensitivity).

32.5 mrad/day by this time. Calculated estimates made using the given parameters resulted in the value of T being 320 days.

The data in Table 1 illustrate well the necessity of simultaneous fulfillment of several conditions for obtaining an SPE contribution to the absorbed dose on the Mir station. For example, event N 38 on 30 October 1992 occurred in the optimal longitudinal interval (the heliolongitude was equal to 61°W), possessed a total flux for the event $J(>30) = 2.05 \times 10^8$ cm^{-2}, but the protons of SPE arrived at the orbit under conditions of a small disturbance of the geomagnetic field ($D_{st} = -37$ nT). The time of the proton flux maximum at the orbit coincided with the passage of Mir station through that part of its orbit most

protected by the geomagnetic field and the contribution to the absorbed dose did not exceed 10 mrad. Event N 7 on 12 March 1989 occurred in the eastern Solar hemisphere (the heliolongitude $-89°$E), the total flux for the event was $J(>30) > 4.74 \times 10^5$ cm^{-2}, but this SPE occurred after a series of other SPEs which "cleaned" the way from the Sun to the Earth (SPE N 6) and protons arrived at the orbit during a considerable geomagnetic storm with $D_{st} = -189$ nT. The time of the proton flux maximum coincided with the MIR station passing through regions near the polar cap and the contribution to the absorbed dose was estimated as 25 mrad.

The estimated absorbed dose was equal to 4460 ± 145 mrad for all SPEs presented in Table 1. At the same time the complete measured absorbed dose was equal to 161,535 mrad, i.e. the SPE contribution was equal to 2.76%. Only on the second day of the SPE on 19 September 1989 was the average daily rate of the absorbed dose exceeded by a factor of 127.

5. Absorbed doses induced by quasi-stable sources

Fig. 1 presents the basic result obtained using the database. Table 2 shows the accumulated absorbed doses during the operational time of each main mission and the daily mean values of the absorbed dose rate determined by D2 channel R-16 dosimeter data (Bondarenko et al., 1995, 2000). Analysis of Table 2 data showed that the daily mean value of the absorbed dose rate anticorrelates with solar activity even using a rough distribution by time. Among all missions one can identify those with high daily mean value of the absorbed dose rate: EO-4, when the largest SPE of the 22nd solar cycle occurred; EO-9, when the SPE series of June 1991 occurred during the phase of the total increase of the daily mean value of the absorbed dose rate (this series contributed additionally to the considered function); EO-15—the operational period of this mission took place during the maximum of absorbed dose variation (see below); EO-19 and EO-20—these missions were carried out during the overall maximum of absorbed dose dynamics which resulted from the maximum of the nearly 11 year variation (close to solar minimum) and the maxima, revealed in further analysis of other, more short-term variations. The daily mean values of absorbed dose in all variations did not exceed permitted radiation levels.

According to the common pattern of the experimental data (Bendat and Pirsol, 1989), the recommended sequence of processes are as follows:

- leading to the zero average value;
- and to a single dispersion;
- trend removal;
- filtration.

In the given case, a different sequence of processes was used. As the contributions to the absorbed dose induced by SPE are stochastic bursts, the data from the everyday routine monitoring of the radiation environment on the Mir station were used for the following analysis. Contributions to the absorbed dose induced by SPE were excluded from this data. When a strong increase in the absorbed dose occurred, caused by arrival at the orbit of radiation induced by an SPE,

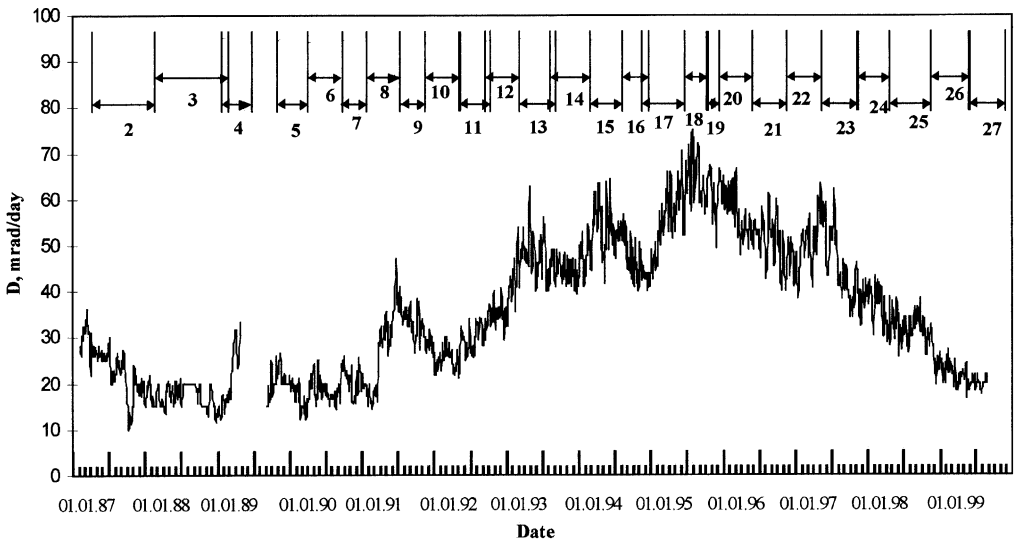

Fig. 1. Dynamics of daily average of absorbed dose rate as indicated by dosimeter R-16 (channel D2). The top of plot shows the numbers of the main missions to the MIR station (2–27).

Table 2
Radiation impact on crews of the main MIR station missions

No.	Missions	Period	$D\Sigma$	D	W
1	EO-2	06.II.87–29.XII.87	7740	23.82	31.77
2	EO-3	21.XII.87–20.XII.88	6495	17.75	95.56
3	EO-4	26.XI.88–26.IV.89	3020	19.87	152.21
4	EO-5	06.1X.89–19.II.90	6975	42.02	161.34
5	EO-6	11.II.90–09.VIII.90	3240	18.00	134.77
6	EO-7	01.VIII.90–10.XII.90	2600	19.70	152.40
7	EO-8	01.XII.90–26.V.91	4285	24.21	138.77
8	EO-9	18.V.91–10.X.91	5415	37.09	157.21
9	EO-10	02.X.91–25.III.92	4975	28.27	136.29
10	EO-11	17.III.92–10.VIII.92	4015	27.31	83.58
11	EO-12	27.VII.92–05.II.93	6800	35.05	74.26
12	EO-13	24.I.93–22.VII.93	8585	47.69	64.32
13	EO-14	01.VII.93–14.I.94	8915	45.25	46.06
14	EO-15	08.I.94–09.VII.94	9505	51.94	29.25
15	EO-16	01.VII.94–06.XI.94	6315	48.95	32.09
16	EO-17	04.X.94–22.III.95	8065	47.44	28.89
17	EO-18	14.III.95–04.VII.95	6745	59.69	17.66
18	EO-19	27.VI.95–11.IX.95	5090	66.10	13.33
19	EO-20	03.IX.95–29.II.96	10980	61.00	11.42
20	EO-21	21.II.96–02.IX.96	10445	53.56	9.12
21	EO-22	17.VII.96–02.III.97	9675	48.86	9.20
22	EO-23	10.II.97–14.VIII.97	9605	51.64	7.60
23	EO-24	05.VIII.97–l9.II.98	7880	39.60	19.51
24	EO-25	29.I.98–25.VIII.98	6990	33.44	83.18
25	EO-26	13.VIII.98–28.II.99	5615	28.08	106.38
26	EO-27	22.II.99–28.VIII.99	3870	20.58	138.06

$D\Sigma$—the accumulated absorbed dose, mrad; D—the daily mean value of the absorbed dose rate, mrad/day; W—the average value of the Wolf number for the exposition time.

it was used as a daily increase in the absorbed dose values obtained during 2–3 preceding days.

Since, as a rule, the R-16 data transmission times did not coincide with the time of ballistic parameter settings, and the orbit multiplicity (the number of days after which the projections of the first day and further orbits coincide or almost coincide) varied from 2 (up to April 1989) to 3 (starting from September 1989), the measurement results were processed using a nonrecursive filter of the form

$$D_i = 1/9(D_{i-2} + D_{I-1} + 3D_i + 2D_{i+1} + D_{I+2}), \qquad (3)$$

where i is the number of the studied day.

The transmission function of this filter is positive everywhere and practically turns oscillations with a period shorter than 4 days into zero. The value of the transmission function is equal to 0.111 at the frequency of 0.25 day^{-1}. The executed processing allowed, on the whole, for the exclusion of sporadic bursts or depressions in the experimental data. In the future the monthly mean values of various functionals obtained using this database will be considered.

Before presentation of statistical results, it is necessary to make a number of provisos. First, for convenience of the analysis of statistical correlations of absorbed dose rate with other parameters, we extended the initial series to include data obtained during the pilotless period of the Mir station lifetime on the basis of the filtration methods (Chemming, 1980). Second, considering the monthly mean values of the absorbed dose rate, Wolf numbers, radio-frequency solar radiation and other space-physics indices as functions of time, we had several realizations concerning stochastic processes. Procedures for statistical estimates are, strictly speaking, applicable to such processes only in the case of their steadiness. As we know in advance that all these processes are unsteady we try to present them as a sum of a determined unsteady part with some addition which will be studied. The unsteady part will be considered as a trend of the studied function during the solar activity cycle. As an example of successful approximation of the solar activity cycle curves in Wolf numbers we present the Hvoikova form (Vitinskiy et al., 1986):

$$W = \frac{W_M}{2}\left[1 - \cos\frac{2\pi t}{\alpha(T_A + T_D) + (1+\alpha)t}\right], \qquad (4)$$

where $\alpha = T_A/T_D$ is the index of the cycle asymmetry, T_A is the duration of the cycle growth phase, T_D is the duration of the cycle depression phase, t is the time from the cycle

beginning, W_M is the maximum value of the Wolf number for the considered cycle, and $T_A + T_D = T_c$ is the duration of the SA cycle.

Since for each solar cycle the values of T_A and T_D are different, formula (4) gives a description of an unsteady eruptive cycle. Choosing October 1986 as the beginning of the 22nd solar cycle, $\alpha = 0.467$, $T_c = 132$ months and November 1996 as the beginning of the 23rd solar cycle, $\alpha = 0.5$, $T_c = 120$ months, we obtain an acceptable approximation of the Wolf number dynamics during the period of the Mir station operation. Treating in a similar way the dynamics of the absorbed dose, it is necessary to remember that the behavior of the radiation sources was caused to a considerable extent by the dynamics of GCR fluxes. During the solar minimum, the GCR fluxes increase and albedo neutron fluxes also increase, decay products of which—protons and electrons—form the ERB. During the solar maximum, solar activity leads to an increase in the atmospheric density, which exercises an increased influence on the ionization deceleration of protons and electrons, resulting in a decrease of the proton fluxes in comparison to those during solar minimum. On the other hand, during solar maximum, the frequency of geomagnetic disturbances increases which causes increasing electron fluxes in the outer zone by diffusion of electrons from regions with a high L value to regions with lower L values. As a result, electron fluxes are increased in comparison to those during solar minimum.

A description of the dynamics of GCR fluxes and the absorbed dose will differ from expression 4. We use the following form (Mitricas, 1999)

$$D(t) = D_1 + D_2\left(\cos\left(\frac{2\pi t}{\alpha T_C + (1-\alpha)t}\right) + D_3 \sin\left(\frac{2\pi t}{T_{CC}}\right)\right), \quad (5)$$

where D_1, D_2, and D_3 are parameters which do not depend on time. D_1 is equal to the partial sum of the absorbed doses for solar minimum and solar maximum periods, D_2 has a meaning of the partial difference of the absorbed doses for solar minimum and solar maximum periods, the product D_3D_2 is the amplitude of the 22-year variation, and T_{cc} is the total duration of two solar cycles. Unlike (4), in this case the beginning of the cycle will be defined by the GCR flux minimum or by the solar maximum. Fig. 2 shows the approximation results of the trend for the absorbed dose dynamics from the D2 channel.

From the approximation procedure it follows that during the period between the maxima of the 21st and 22nd solar cycles, where some values of parameters for (5) are used, the essential influence was exercised on the dynamics of monthly mean values of the absorbed daily dose rate by frequent corrections of the station orbit altitude and rather low values of average altitudes before September 1989 in comparison with the period after September 1989, when other values of parameters are used (5). Using calculational models where a dependence of the absorbed dose rate on the altitudes is taken into consideration, one can expect a better description of the trend in the time interval before September 1989.

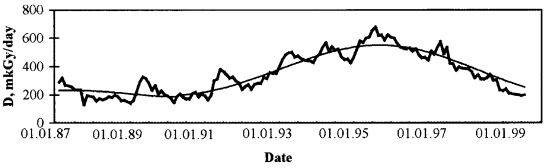

Fig. 2. Approximation (solid thin line—trend) according to formula (5) of the monthly average daily rate of the absorbed dose (solid bold curve), measured on the MIR station.

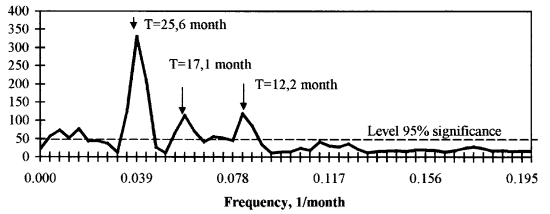

Fig. 3. Spectral density of power RD (t).

Fig. 2 shows the trend approximation (the solid thin curve) by formula (5) of the monthly mean values of the absorbed daily dose rates (the solid thick curve), measured on the Mir station. From analysis of Fig. 2 data it follows that the differences between experimental monthly mean values of absorbed doses and the approximation trend RD(t) can contain several variations. For examination of this assumption, we calculated the spectral density of the power RD(t), although the executed analysis showed that the RD(t) function does not comply with the criteria of steadiness. An estimation of the spectral density of power was made by the method of Blackman–Tjuky using the Hemming smoothing window (Marpl-Yn, 1990). Fig. 3 shows the results of the calculations. From Fig. 3 it follows that search of variations can be made for three frequencies (or periods) $V = 0.0391$; 0.0820 month (-1) ($T = 25.6$, 17.1 and 12.2 months). It is known from (Vampola, 1990) that the majority of periodicities with $T < 11$ years, discovered through displays of solar activity, have an unstable character over 2–3 solar cycles. For examination of the steadiness of the discovered frequencies (periods) of RD(t) variations we made a spectral time analysis consisting of the densities of the power spectra that were calculated, using a 5 years long database with a shift of the start of reading by 0.25 years (3 months). For convenience Fig. 4 shows the dynamics of locations of peaking variations of power spectrum density RD(t) as a function of the interval for which the calculations were made.

The analysis of peak period dynamics gives the following mean values of variation periods: $T1 = 24.46 \pm 2.47$ months,

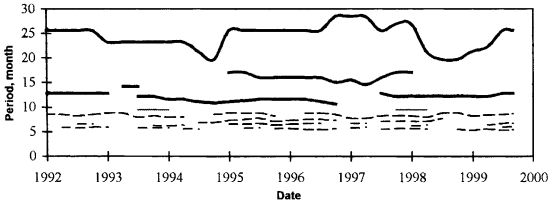

Fig. 4. Dynamics of positions of peak periods for spectral density of power RD (t).

$T2 = 15.81 \pm 0.97$ months, and $T3 = 12.01 \pm 0.65$ months. Values of variation periods are close to values obtained from the power spectrum density. Besides the second variation having a rather high peak, the power spectrum density appeared only 16 times among the 32 intervals considered, was absent until 1995 and disappeared again after 1998. It is possible that a unique feature of the 22nd solar cycle displays itself in this variation, or it may be that neglected dynamics of the orbit altitude variations during the beginning of the considered time interval showed itself just at this point. The third variation did not reveal itself in 1997,00–1997,25. The other variations ($T \approx 8.6$, 7.3, 6.5, 5.7, and $\leqslant 5.0$ months) also did not reveal themselves during the whole considered time interval and amplitudes of these variations have a background level. Besides the considered peaks of the power spectrum density, its remaining part can be safely interpreted as low-frequency white noise.

If we try to find a physical interpretation for the discovered variations, for the close of the 2-year variation there is a good similarity with the large-scale variations of cosmic rays and solar activity (Lyubimov, 1980), and the close of the 1-year variation is most likely caused by variations of the atmosphere density. The so-called "seasonal variations" (Teltsov et al., 1997) are determined by the fact that the high atmosphere density, which determines the mechanism of ERB particles losses in the SAA region at altitudes of 400–500 km, varies essentially from winter to summer. However, this variation is irregular, differing from 1 year to the next and from one solar cycle to the next and, therefore was accounted for inadequately in standard programs of atmosphere density calculations (SS 25645.115, 1985).

Considering correlation of the absorbed dose rate dynamics with mean values of the atmospheric density, we determined from data for the complete observation period that the correlation coefficient is rather high: equal to 0.778. The correlation function reaches the extreme value by delaying of the absorbed dose rate with respect to the atmospheric density by 10.5 months. Table 3 presents the correlation coefficient values and the extreme values of correlation functions of the absorbed dose rate with the space-physical indices and the parameters of the Mir station flight path. Fig. 5 shows graphs of correlation functions of the absorbed dose rate with the same parameters, but only in the delay region (negative shift), since forecasting each parameter with respect to the absorbed dose rate is of interest. Reaching an extreme of the correlation function of several parameters calls attention by delaying in the interval by 10–12 months. As was expected, positive correlation is observed with GCR fluxes and a negative correlation is observed with the direct indices of the solar activity—Wolf numbers and the radio-frequency flux. It is possible that the practical coincidence of delaying values for galactic and solar indices is an expression of unusual features of the 22nd solar cycle. If we consider the correlation function of GCR proton fluxes and the Wolf number, one can see that the correlation maximum (0.929) is reached when GCR fluxes precede the Wolf number by 1 month. For the same time, when the delay was equal to zero, the correlation coefficient was equal to 0.922 (strictly speaking, these values are not statistically distinguishable). Low correlation of the absorbed dose rate is noticed even when considering the delay of the geomagnetic indices. This can probably be explained by the fact that the geomagnetic field has the greatest effect on electron fluxes, which make a much smaller contribution to the absorbed dose inside the Mir station in comparison to other sources. The geomagnetic situation heavily influences protons during occurrence of SPEs, but in our analysis the

Table 3
Statistical estimates for correlation of the absorbed dose rate with various parameters

No.	Parameter	Correlation coefficient	Extreme value of correlation function	$-\Delta t$, month	Line regression equation D
1	W	−0.714	−0.861	11.0	$3.30 + 0.423W$
2	$F_{10,7}$	−0.675	−0.894	12.0	$-20.18 + 0.432F_{10,7}$
3	$J_{>90}$	0.686	0.886	11.0	$26.63 + 3.886J_{>90}$
4	D_{st}	0.214	0.371	15.0	$45.35 + 0.498D_{st}$
5	A_P	−0.141	−0.589	20.0	$27.43 + 0.549A_p$
6	H_{IOAA}	0.601	0.601	0.0	$-216.69 + 0.643H_{IOAA}$
7	ρ	−0.778	−0.830	10.5	$27.80 + 1.878\rho$
8	$1/\rho$	0.850	0.885	10.0	$32.54 + 5.139/\rho$

Δt—delay for extreme value of correlation function.

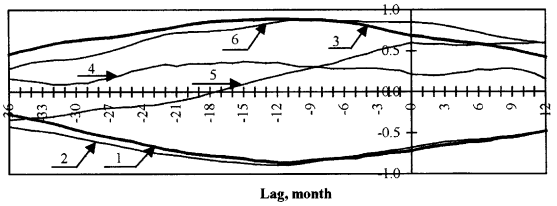

Fig. 5. Correlation functions of the absorbed dose rate with various parameters: 1—Wolf numbers (W); 2—radio-frequency solar flux with the wave length 10.7 cm ($F10.7$); 3—GCR proton flux at the energy above 90 MeV ($J > 90$); 4—D_{st}-variation amplitude; 5—station's orbit altitude during passing the South Atlantic Anomaly (H_{SAA}); 6—the inverse density of the atmosphere in SAA zone.

SPE proton contribution was excluded. Therefore, one can conclude that disturbances of the geomagnetic situation weakly influence the absorbed dose inside the Mir station (when considering crew activity outside the station, it is necessary to take into account geomagnetic disturbances, because they influence electron fluxes which can penetrate the astronauts space suit).

The basic conclusions of this analysis are as follows: (a) the forecasting value of the regressive correlation, presented in Table 3, is rather limited. All obtained correlations depend on the calendar time and on the date series length which is to be used for forecasting; (b) obviously in the case of Mir station flight at different altitudes, the coefficients of linear regression equations should be different; (c) the natural desire is to study the correlation of the absorbed dose rate with the orbit altitude or with the altitude in the SAA zone. The attempt to find dose–altitude correlation for short intervals of time (Mitricas, 1990) was unsuccessful. Correlation coefficients demonstrate considerable variations from -0.7 to $+0.7$ and their behavior depends on the time interval length during which the correlation dependence is studied, i.e. the orbit of a spacecraft has to be taken into consideration by direct methods of calculations.

The formation of techniques of the absorbed dose dynamics forecasting using only statistical correlation is doomed to failure. But by developing forecasting techniques that consider the position of spacecraft orbit in space, it was discovered during the present analysis that it is necessary to take into account different variations of the absorbed dose rate caused by variations of the space-physical indices.

6. Conclusions

1. For the first time in the history of using onboard instrumentation for dosimetric monitoring, a long-term data series (for a time period exceeding the solar cycle duration) of the daily absorbed dose inside the orbital station modules was obtained.

2. According to results of the correlation analysis for this database, we established that the dynamics of the daily mean absorbed doses correlate well with parameters of the solar activity (the Wolf number, W) and with parameters determining the high-altitude atmospheric density (the $F_{10.7\ cm}$ index), and that there is almost no correlation with variations of the geophysical parameters determining the magnetospheric conditions.

3. During the 22nd solar cycle, the "seasonal" variations of the absorbed dose rate were clearly observed. These variations significantly exceeded the ones calculated, using standard model values, and are caused basically by changes in the high-altitude atmospheric density.

4. Despite the total contribution of SPE protons to the integral dose (during the total period of Mir station utilization) being smaller than several percent, during unfavorable conditions (intensive fluxes, hard spectrum, large D_{st}, station passages through polar caps during SPE maxima, etc.) the absorbed dose rate in the inhabited modules of the station for tens of minutes can reach hundreds of mrad/min (on 20 October 1989 the mean absorbed dose rate according to R-16 measurements reached 30 mrad/min). In such cases the role of forecasting the radiation situation evolution and measures directed to decreasing the radiation in risk of crew members decreases.

5. Using long-term measurements, we discovered that, in spite of variations in the limits of one order of the absorbed dose value induced by space radiation inside compartments of the orbital station, these doses are in the region of very low range and only exceed by a factor of 2–3 the Earth's natural background. At the present time doses are attributed to the region of the radiation hormesis which allows us to expect metabolic process intensification inside cells of living organisms, plants and microflora on the orbital station.

References

Bendat, D., Pirsol, A., 1989. Applied Analysis of Random Process. MIR, Moscow, p. 540.

Bondarenko, V.A., Mitricas, V.G., Tsetlin, V.V., 1995. Solar activity variation and radiation situation onboard MIR station from 3986 to 1984. Air-Space Biol. Ecol. Med. 29 (6), 64–67.

Bondarenko, V.A., Mitricas, V.G., Tsetlin, V.V., 2000. Radiation environment of OC MIR during minimum of the 22nd solar cycle (1994–1996). Air-Space Biol. Ecol. Med. 34 (1), 21–24.

Chemming, P.V., 1980. Numeral Filters, Sovets. Radio. Moscow Publishing House, p. 224.

Kovalev, E.E., Kolomensky, A.V., Petrov, V.M., 1986. Radiation safety provision. In: Gurovskiy, N.N. (Ed.), book: Medical Research Results, Made Onboard Orbital Scientific-Research Complex "Salyut-6"—"Soyuz". Moscow Publishing House "Nauka", Moscow, pp. 54–75.

Lyubimov, G.P., 1980. The large-scale variations of cosmic rays and solar activity. Izv. AN USSR Ser. Phys. 44 (12), 2588–2609.

Marpl-Yn., 1990. Numeral Spectral Analysis and its Supplements. MIR, Moscow, p. 584.

Mitricas, V.G., 1990. A model of Earth's radiation belts for estimation of particles. Air-Space Equipment (8), 32–48.

Mitricas, V.G., 1999. Radiation situation in the orbit region of MIR station. Kosm. Issledov. 37 (5), 1–5.

Mitricas, V.G., Tsetlin, V.V., 1995. Large-scale variations of radiation situation onboard MIR station. Kosm. Issledov. 33 (4), 389–394.

Mitricas, V.G., Tsetlin, V.V., 2000. The problem of security of radiation safety on OC MIR in the 22nd solar cycle. Kosm. Issledov. 38 (1), 1–6.

RD 50-25645223, 1991. Methodical Instructions. Radiation Safety of Spacecraft Crew during Cosmic Flight: Examination of a System of Radiation Safety Provision During Flight. Moscow Publishing House Standards, p. 12.

Sawyer, D.H., Vette, J.I., 1976. AP-8 trapped proton environment for solar maximum and solar minimum. MSSDS/WDC-A-R & S, NASA-TM-X-72605. December, p. 176.

SS 25645.115, 1985. The upper Earth's atmosphere. A Model of the Density for Ballistic Provision of Artificial Earth's Satellites Flights. Moscow Publishing House Standards, p. 44.

SS 25645.135, 1987. Natural Earth's radiation belts. Space Energy Characteristics of Electron Fluxes. Moscow Publishing Housed Standards, p. 60.

SS 25645.138, 1987. Natural Earth's radiation belts. Space Energy Characteristics of Proton Fluxes. Moscow Publishing House of Standards, p. 50.

State Standard (STST) 25645.215, 1985. Radiation safety of spacecraft crew during cosmic flight. Safety Standards by Flight Duration up to 3 years. Moscow Publishing House of Standards, p. 4.

Teltsov, M.V., Shumshurov, V.I., Tsetlin, V.V., 1997. Radiation dose variations onboard MIR station under Geophysical conditions changes. MSU's Bull. Phys. Ser. Astron. (1), 47.

Tverskay, L.V., Teltsov, M.V., Shumshurov, V.I., 1991. Radiation Dose Measurements onboard MIR Station during solar proton events in September–October, 1989. Geomagnetizm i Aeronomia (5), 928–930.

Vampola, A.L., 1990. Solar Cycle Influence on Trapped Energetic.

Vernov, S.N. (Ed.), 1983. Cosmic Space Model (Cosmos Model-82), Vol. 3. MSU Publishing House, Moscow, p. 635.

Vitinskiy, Y.I., Kopetskiy, M., Kuklin, G.V., 1986. Statistics of Spot-Formation Activity of the Sun. Nauka, Moscow, p. 296.

Yuraytin, E.I., Shumshurov, V.I., Fominich, V.A., Teltsov, M.V., 1979. A study of dosimetric characteristics of a ionization chamber with an electrostatic relay. Measuring Equipment (3), p. 48.